Send Orders for Reprints to reprints@benthamscience.net

Current Applied Polymer Science, 2020, *4*, 1-00

RESEARCH ARTICLE

Fabrication and Mechanical Properties of POSS Coated CNTs Reinforced Expancel foam core Sandwich Structures

Wanda Jones[1], Bedanga Sapkota[1], Brian Simpson[1], Tarig A. Hassan[1], Shaik Jeelani[1] and Vijaya Rangari[1,*]

[1]*Department of Materials and Science Engineering, Tuskegee University, Tuskegee, AL36088*

Abstract: ***Background*:** Sandwich structures are progressively being used in various engineering applications due to the superior bending-stiffness-to-weight ratio of these structures. We adapted a novel technique to incorporate carbon nanotubes (CNTs) and polyhedral oligomeric silsesquioxanes (POSS) into a sandwich composite structure utilizing a sonochemical and high temperature vacuum assisted resin transfer molding technique.

***Objective*:** The objective of this work was to create a sandwich composite structure comprising of a nanophased foam core and reinforced nanophased face sheets, and to examine the thermal and mechanical properties of the structure. To prepare the sandwich structure, POSS nanoparticles were sonochemically attached to CNTs and dispersed in a high temperature resin system to make the face sheet materials and also coated on expandable thermoplastic microspheres for the fabrication of foam core materials.

***Methods*:** The nanophased foam core was fabricated with POSS infused thermoplastic microspheres (Expancel) using a Tetrahedron MTP-14 programmable compression molder. The reinforced nanophased face sheet was fabricated by infusing POSS coated CNT in epoxy resin and then curing into a compression stainless steel mold.

***Results*:** Thermal analysis of POSS-infused thermoplastic microspheres foam (TMF) showed an increase in thermal stability in both nitrogen and oxygen atmospheres, 19% increase in thermal residue were observed for 4 wt% GI-POSS TMF compared to neat TMF. Quasi-static compression results indicated significant increases (73%) in compressive modulus, and an increase (5%) in compressive strength for the 1 wt% EC-POSS/CNTs resin system. The nanophased sandwich structure constructed from the above resin system and the foam core system displayed an increase (9%) in modulus over the neat sandwich structure.

***Conclusion*:** The incorporation of POSS-nanofillier in the foam core and POSS-coated nanotubes in the face sheet significantly improved the thermal and mechanical properties of sandwich structure. Furthermore, the sandwich structure that was constructed from nanophased resin system showed an increase in modulus, with buckling in the foam core but no visible cracking.

ARTICLE HISTORY

Received: July 16, 2020
Revised: September 28, 2020
Accepted: October 12, 2020

DOI:
10.2174/2452271604999201123193149

Keywords: Expancel foam, CNTs, POSS, Sandwich Structure, thermal properties, mechanical properties.

1. INTRODUCTION

Sandwich structures have been used in aerospace, automotive, and transportation applications due to incredibly lightweight, high noise absorption, and stiffness features. Composite sandwich structures consist of three main parts: two thin, stiff, and strong faces separated by a thick, light, and weaker core. Sandwich panel face sheets are the outer layers of the sandwich structure and are usually constructed from glass or carbon fibers and a polymer based resin. In a sandwich, the face sheets carry most of the load as they are stiffer and stronger, while the lightweight core separates the face sheets so that a higher bending stiffness of the composite plate can be achieved. Polymer matrix composites are one of the most common face materials used for sandwich structures. These materials use a polymer based resin as a matrix material with some form of fibers embedded in the matrix, as reinforcement. Both thermosetting and thermoplastic polymers can be used for the matrix material. Common polymer composite thermosetting matrix materials include polyester, vinyl ester and epoxy [1-4].

The core also plays an important role in enhancing the energy absorption capability during an impact by internally

* Address correspondence to this author at the Department of Materials and Science Engineering, Tuskegee University, Tuskegee, AL 36088;
E-mail: vrangari@tuskegee.edu

2452-2716/20 $65.00+.00

dampening the impact energy as the stress waves propagate. The core determines the extent of damage in a sandwich composite. The core materials are often composed of balsa wood, various types of honeycomb structures, lingo-cellulosic resources, and foam [5-7]. Each core has various advantages and drawbacks. For example, balsa wood is a lightweight core with high strength, but can rot or mold with exposure to moisture. Honeycomb material is strong and stiff, but is often more expensive and it can be tricky to achieve a quality bond between the face sheets and core. Foam is usually not as stiff as balsa, but is impervious to moisture and has good insulating properties. Overall, the core gives structure to the sandwich, and the face sheets protect the core [3]. Sandwich structures commonly use thermoplastic foams as core materials. Properties of thermoplastic foams include an extremely low density, good insulating properties, energy absorption, and relatively low cost, making thermoplastic foams good candidates for applications in boats, ships, high-performance aerospace vehicles, rail cars, surfboards, and wind energy structures [1].

In recent years, researchers have placed emphasis on improving the properties of polymers and polymeric foam materials by the addition of small amounts of nanoparticles such as carbon nanotubes, nanofibers, TiO_2, SiC, and nanoclays [8-13]. Nanomaterials-infused polymeric composites have gained interest due to their unique behavior in mechanical and thermal properties over their pristine counterparts. Recent studies have reported that nanoparticle-infused polymer systems exhibit higher energy absorption capacity, enhanced mechanical and thermal properties compared to pure polymer systems [14, 15]. Mahfuz *et al*. used acoustic cavitation to infuse SiC and TiO_2 nanoparticles into polyurethane foams [10-13]. These nanophased foams exhibited an increase in thermal stability, strength, and stiffness under flexural loading. We have shown that the infusion of closite clay in phenolic foam increases the thermal and compressive properties [16, 17].

Over the past few decades, carbon nanotubes (CNTs) have received major attention as components of polymer-based nanocomposites. CNTs have been used as high strength, low weight nano-reinforcements for composites [18, 19]. However, the poor dispersal properties of CNTs in polymer resins and the weak interfacial bonding of CNTs with polymer matrices have hampered the scope of CNT applications in practical devices [20, 21]. Therefore, modification of the CNT surface and good dispersion of CNTs is required for industrial applications. Research in these areas has focused on functionalization as a strategy to enhance both dispersion and interfacial bonding. Methods that have been used have involved covalent and noncovalent reactions that included chemical modification using oxidation, direct-fluorination, and amino-functionalization, and surface coating with various nanofillers as well as polymer wrapping of CNTs [22-31].

Polyhedral Oligermic Silsesquioxanes (POSS), with general structure of silicon-oxygen cage surrounded by organic R group, are inorganic-organic hybrid materials that have received attention as a promising material. Silsesquioxanes are organic silica compounds with the general formula being ($R\text{-}SiO_{1.5}$). POSS nanoparticles have diameters from one to three nanometers and are analogues to the smallest possible particles of silica. The characteristics and surface reactivities can be altered by changing the functional groups (R) on a POSS molecule. Possible functional groups include almost any organic group such as methyl, isobutyl, cyclopentyl, or cyclohexyl. This variety in functionalization is the source of one of the main differences between POSS molecules and customary fillers. Most nanoparticles, including CNTs, are characteristically inert and have no direct interaction with the polymers they fill. However, most of the inorganic nanoparticles are surface modified to promote interactions and compatibility with the polymer. Infusion of covalently attached POSS in polymers results in higher glass transition temperatures (T_g) as well as increased hardness, toughness, fire-retardance, and corrosion inhibition [32-37].

In this work, POSS nanoparticles were sonochemically attached to multi-walled carbon nanotubes and dispersed in a high temperature epoxy resin system for the face sheet materials and POSS nanoparticles were sonochemically attached to expandable thermoplastic microspheres and fabricated into foam core materials. A sandwich structure was constructed from the above resin and foam core systems that exhibited significant improvement in properties as compared to its constituents.

2. MATERIALS AND METHODS

2.1. Materials

Multi-walled carbon nanotubes (CNT, 10-20 nm in diameter and 0.5-20 μm in length) were purchased from Nanostructured & Amorphous Materials Inc, USA. POSS nanomaterials EpoxyCyclohexyl (EC) POSS, and GlycidylIsooctyl (GI) POSS were bought and used as received from Hybrid Plastics, USA. The microspheres used in this research were Expancel-092-DU-120, this dry unexpanded thermoplastic polymer (particles sizes 28-38μm) was received from Expancel Inc. The polymeric matrix used in this investigation was commercially available RenInfusion 8612 epoxy resin, obtained from Freeman Manufacturing and Supply. RenInfusion 8612 is a one-component, low-viscosity epoxy system developed for use in the production of advanced composites using vacuum-assisted resin transfer molding (VARTM), resin transfer molding (RTM), Seemans Composite Resin Injection Molding Process (SCRIMP^{sm}), and other infusion processes. Hexane was used as a solvent in the ultrasonic irradiation steps and was purchased from Sigma-Aldrich.

2.2. Fabrication of Face Sheet Materials

2.2.1. Preparation of POSS Nanofiller Coated CNTs

The processing of the neat, EC- and GI-POSS coated CNTs was as follows. One gram of POSS nanofiller and 1g of CNTs were mixed in 70 ml of n-hexane and irradiated with a high intensity ultrasonic horn for 3 hours at 5^{o}C. The

reaction product was thoroughly washed with double distilled water and then with pure ethanol. Finally, the products were centrifuged at 10000 rpm and vacuum dried overnight at room temperature.

2.2.2. Fabrication of a POSS Nanofiller Coated CNT-Infused Epoxy Resin System

Prior to curing, the RenInfusion 8612 epoxy resin was mixed with known weight percentages of the different POSS coated CNTs (0.5 and 1 wt %) using a Thinky hybrid defoaming mixer ARE-250 for 30 minutes. The final reaction mixture was transferred into a compression stainless steel mold for curing. The neat and nanophased samples were cured at 93°C for 16 hours then post cured at 149°C for an additional 2 hours in a mechanical convection oven. The mold was allowed to cool to room temperature and the specimens were removed from the mold, machined for smoothness, and then assessed for thermal and mechanical characteristics.

2.3. Fabrication of Foam Core Materials

2.3.1. Preparation of POSS Nanoparticle Coated Expandable Thermoplastic Microspheres

The coating of expandable thermoplastic polymeric microspheres (TPMs) with POSS nanofiller was as follows. Three weight fractions of 2%, 4% and 6% were prepared by adding 2, 4, and 6 g of POSS nanoparticles to 98, 96, and 94 g, respectively, of TPM and mixed with 150 ml of n-hexane. The mixtures were irradiated with a high intensity ultrasonic horn (Ti-horn, 20 kHz - 100 W/cm^2) for 30 minutes, the reaction temperature was maintained using a circulated coolant chiller at 5°C. The samples were vacuum dried at room temperature for 12 hours and oven dried at 60°C for 1 hour to remove excess hexane that remained in the mixture.

2.3.2. Fabrication of Neat and Nanophased Foam Core Materials

The POSS infused TPMs were fabricated into a foam core panel using a Tetrahedron MTP-14 programmable compression molder by heating to 190°C for 15 min under a pressure of 15000 lbs. Molds were cooled to room temperature to remove the foam core panel. The samples were cut to the required dimensions for thermal and mechanical characterization.

2.4. Thermal Analysis

2.4.1. Thermogravimetric Analysis

In order to measure thermal stability of both face sheet and foam core materials, thermogravimetric analysis (TGA) was carried out on a Mettler Toledo TGA/SDTA 851e under both nitrogen and oxygen rich atmospheres. Face sheet and foam core samples ranged in weight between 10–15 mg. The samples were heated to 800°C from room temperature at a heating rate of 10°C/minute.

2.4.2. Thermo Mechanical Analysis

Thermo mechanical analysis (TMA) of face sheet materials was carried out on a TMA 2940 (Manufacturer: TA Instruments, Newark, DE). The samples were cut into small pieces of dimensions 5 mm x 5 mm x 5mm using a diamond cutter and machined using a mechanical grinder to maintain the specified sample dimensions according to the standard ASTM E 831-06 [35]. Dimensional changes were measured in the thickness direction. The temperature was ramped from 25 to 160°C at a rate of 5°C/minute.

2.5. Mechanical Analysis by Quasi-Static Compression

In order to investigate the quasi-static compression response, the specimens were tested according to ASTM C 365-03 standard [39]. Experiments for the foam core materials were conducted on a 2.5 kN Zwick Roell Z 2.5 machine equipped with TestXpert data-acquisition system. The machine was operated under displacement control mode at a crosshead speed of 2.0 mm/minute, and all tests were performed at room temperature. In order to investigate the quasi-static compression response of the neat and nanophased resin systems, as well as the final sandwich structure, the specimens were tested in the thickness direction using a servo-hydraulically controlled Material Testing System (MTS) machine. The capacity of the MTS machine was approximately 10 kN. The test was carried out in displacement control mode and the crosshead speed was 0.125 mm/s.

2.6. Final Sandwich Composite Structure

2.6.1. Fabrication of sandwich structure

The fabrication of the neat and nanophased sandwich composites was carried out using a High Temperature Vacuum Assisted Resin Infusion Molding. The details of the construction are illustrated in Fig. (**1**). In this study, we have used eight layers of satin weave carbon fiber 3.5 in x 5 to achieve the required thickness of the composite. The following sequence was followed to fabricate the neat and nanocomposite structures. Initially, a release ply porous Teflon 10 in x 10 in and breather fabric was placed on a glass sheet. On top of the breather fabric a heating blanket that measured 10 in x 10 in and non-porous Teflon was applied on top of the heater blanket. A 3.5 in x 5 in an aluminum sheet with thermocouples wrapped in non-porous Teflon was applied to the layer. Porous Teflon and four layers of the carbon fabric were placed on the aluminum sheet. The core was then placed, followed by the other four layers of carbon fabric. Another non-porous Teflon sheet and then a distribution mesh (to achieve uniform distribution of the resin) were placed on top of the fabric. A piece of spiral wrapping was placed on the opposite sides of the carbon fibers and clear tubing was attached and sealed to one end of each spiral wrapping. One tube (resin inlet) covered the mesh and bonded with an adhesive spray. The entire system was enclosed within the vacuum bagging in conjunction with RenInfusion

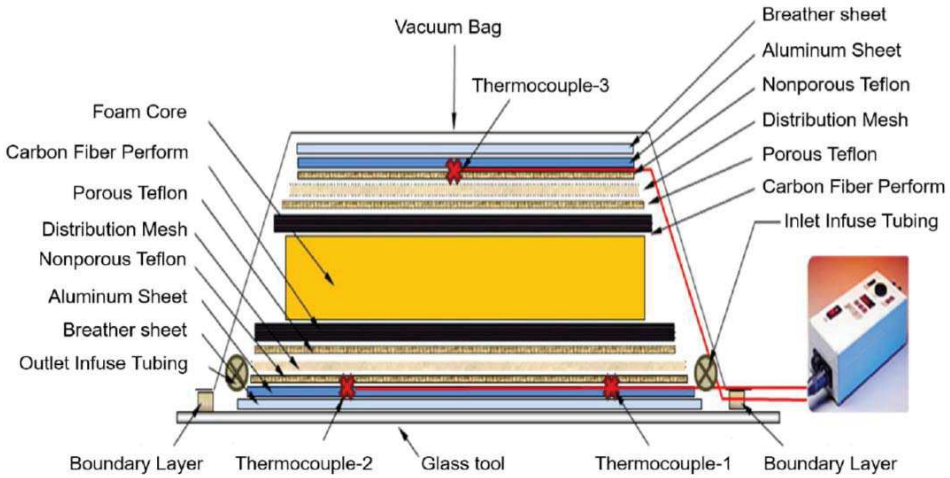

Fig. (1). Schematic diagram showing fabrication of a sandwich nanocomposite structure. (*A higher resolution / colour version of this figure is available in the electronic copy of the article*).

resin injection and ejection tubing. The resin inlet tube was clamped and placed into a 1-liter container of resin and the resin outlet tube was attached to a trap in conjunction with tubing attached to a vacuum pump (approximately 711.2 mm Hg); the system was debulked (removal of air) for approximately 30 minutes. The clamp to the resin inlet tube was released and the resin was infused for a period of ~30 minutes to 1 hour). After infusion, the resin inlet tubing was re-clamped and the pump was left on to allow excess resin to be extracted. This system does not cure at room temperature; thus, the entire vacuum-bagged composite resin system was cured at 93ºC for 16 hours using a Witchitech HB-1 Hot bonder with thermocouples to monitor the system temperature throughout the process and a heating blanket as the heating source.

2.6.2. Optical Microscopy of Sandwich Nanocomposite

Optical observations were performed using a Nikon Optical Microscope by Excell Technologies.

3. RESULTS AND DISCUSSION

3.1. Thermal Analysis

To test thermal stability of neat TMF and various percentages of EC-POSS and GI-POSS infused TMF, TGA in nitrogen and oxygen atmospheres were studied. These experiments were performed to determine the changes in weight loss in relation to change in temperature and atmospheres.

3.1.1. Thermal Characterization of Neat TMF and POSS Infused TMF in Nitrogen Atmosphere

(Fig. **2a-d**) depict the TGA curves for neat TMF and 2, 4, and 6 wt% of EC-POSS reinforced TMF, respectively; the results are summarized in Table **1**. With the incorporation of EC-POSS, the first weight loss of the neat TMF (due to the loss of organic vapor) was delayed by 54°C. The second weight loss at 299 °C is attributed to the decomposition of the polymer, which is shifted to 303 °C, 309 °C, and 311 °C with 2, 4, and 6 wt% loading of EC-POSS, respectively. The decomposition of the polymer step was increased by 12°C for 6 wt% EC-POSS infusion. The increase in thermal residue was 6 and 8 wt%, respectively, for 2 and 4 wt% EC-POSS compared to the neat TMF.

(Fig. **3a-d**) depict the TGA curves of neat TMF and 2, 4, and 6 wt% of GI-POSS reinforced TMF, respectively; the results are summarized in Table **1**. Among these reinforced composite foams, the 2 wt% GI-POSS TMF exhibited the highest thermal residue at 41wt%. The first decomposition step for 2 wt% GI-POSS TMF increased by 45^{o}C compared to the neat TMF. The 6 wt% GI-POSS TMF had the highest increase in the first decomposition step of 69 ^{o}C.

3.1.2. Thermal characterization of neat TMF and POSS infused TMF in oxygen atmosphere

Thermal oxidative degradation of plastics at elevated temperatures is an inevitable event and for many polymers this degradation can significantly limit the application service life of a product [40]. Despite this limitation, the use of a base polymer that is naturally highly resistant to thermal degradation will enable plastic products to be used at elevated temperatures with confidence that these plastic products will work as designed [41]. If the use of a naturally resistant polymer is not possible, then the correct selection and use of a relevant stabilizer package can also considerably extend the service life of a polymer. This is especially important in the case of polymer foam core sandwich composites. To test the thermal oxidative stability of neat TMF and various percentages of EC-POSS or GI-POSS infused TMF composites, TGA with an oxygen atmosphere was studied. These experiments were performed to determine the changes in weight loss in relation to change in temperature and oxygen atmosphere.

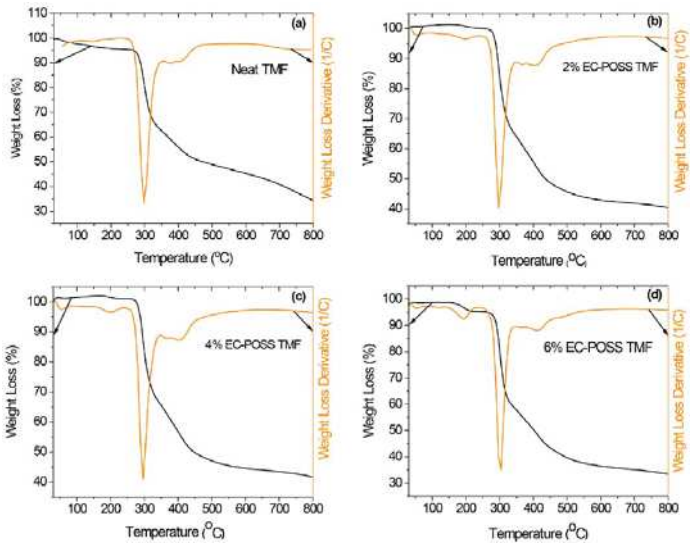

Fig. (2). TGA curves of (**a**) neat TMF (**b**) 2% EC-POSS TMF (**c**) 4% EC-POSS TMF, and (**d**) 6% EC-POSS TMF. (*A higher resolution / colour version of this figure is available in the electronic copy of the article*).

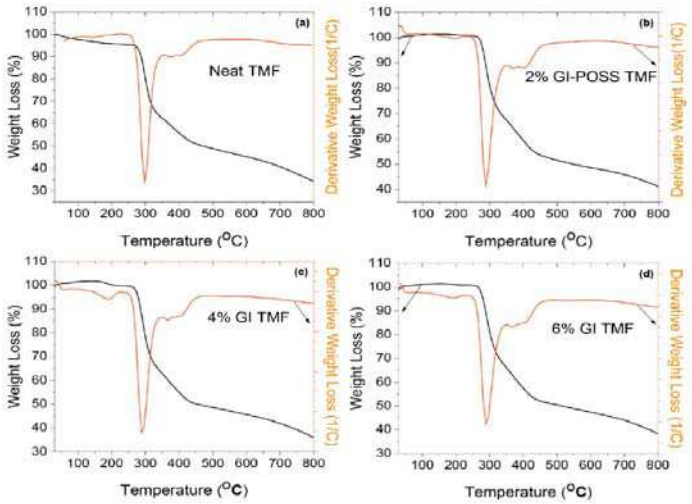

Fig. (3). TGA curves of (**a**) neat TMF (**b**) 2% GI-POSS TMF (**c**) 4% GI-POSS TMF, and (**d**) 6% GI-POSS TMF. (*A higher resolution / colour version of this figure is available in the electronic copy of the article*).

Table 1. TGA data for neat, EC-POSS and GI-POSS TMF.

	T_{dec}(°C)			
Sample	**First**	**Second**	**Third**	**ΔW (% at 800°C)**
Neat TMF	147	299	406	34
2% EC- POSS TMF	-	303	(12)	555(61)
4% EC- POSS TMF	-	309	(15)	532(55)
6% EC- POSS TMF	195	311	(8)	523 (57)
2% GI- POSS TMF	197	290	409	41
4% GI- POSS TMF	191	291	408	36
6% GI- POSS TMF	192	292	409	38

(Figs. **4a**, **4b**, **4c** and **4d**) show the TGA curves of neat TMF and 2, 4, and 6 wt% infusion of EC-POSS in TMF obtained in an oxygen atmosphere, respectively; the results are summarized in Table **2**. The first weight loss related to organic vapor evaporation completely disappeared with neat TMF and 2 wt%-6 wt% EC-POSS TMF. The second weight loss temperature, which is determined from the peak of the derivative curve, decreased (303°C) by the addition of 2wt% EC-POSS and was regained by addition of 6 wt% of EC-POSS in TMF. The decomposition of the polymer step increased by - 13°C for 2 wt% of EC-POSS infusion and decreased by 19°C for 6 wt% of EC-POSS infusion in TMF. The thermal residue increased from 11 to 18 wt% for 2 wt% and 4 wt% infusion of EC-POSS as compared to the neat TMF.

(Figs. **5a**, **5b**, **5c** and **5d**) show the TGA curves obtained in oxygen atmosphere for neat TMF and 2%, 4% and 6% GI-POSS infused TMF, respectively; the results are summarized in Table **2**. As stated earlier, the loss of organic vapor step completely disappeared for neat and 2 wt% GI-POSS TMF. The second weight loss temperature decreased (307°C) by the addition of 2wt% GI-POSS. With the addition of 4 wt% of GI-POSS in TMF, the weight loss temperature returned to 314°C. The decomposition of the polymer step decreased by 15°C for 2 wt% and increased by 18°C for 4 wt% GI-POSS TMF. The thermal residue increased from 12 to 19 wt% for 2 to 4 wt% GI-POSS TMF compared to the neat TMF. The 4% GI-POSS TMF exhibited the highest thermal oxidative residue of all TMF specimens.

3.2. Thermo mechanical analysis (TMA)

Table **3** summarized the TMA results of neat TMF and EC-POSS infused TMF. These results clearly show a 118

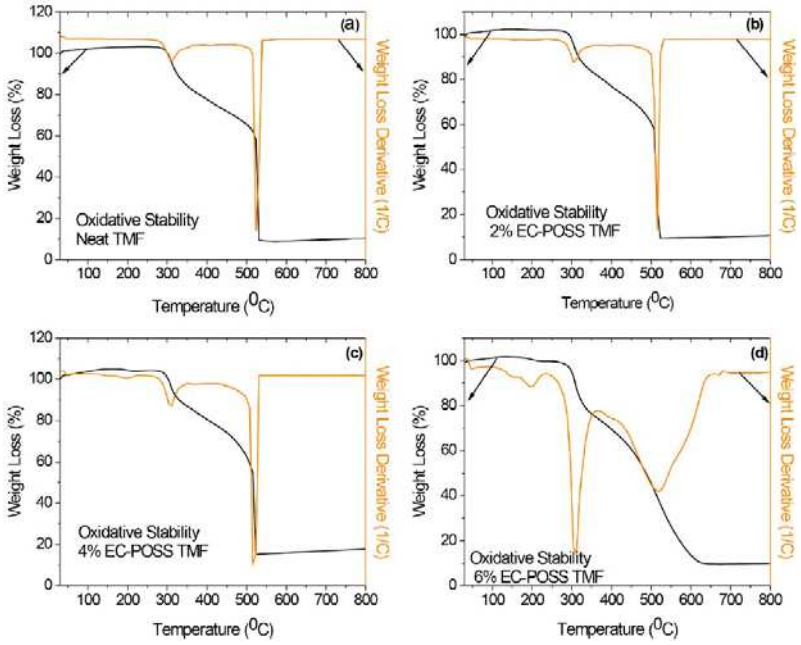

Fig. (4). Thermal oxidative stability curves for (**a**) neat TMF (**b**) 2% EC-POSS TMF (**c**) 4% EC-POSS TMF, and (**d**) 6% EC-POSS TMF. (*A higher resolution / colour version of this figure is available in the electronic copy of the article*).

Table 2. Thermal oxidative stability data for neat, EC-POSS and GI- POSS TMF.

	T_{dec}(°C)				
Sample	**First**	**Second**	**Weight Loss**	**Third**	**ΔW (% at 800°C)**
Neat TMF	-	311	(13)	542	10
2% EC- POSS TMF	-	303	(12)	555	11
4% EC- POSS TMF	-	309	(15)	532	18
6% EC- POSS TMF	195	311	(8)	523	10
2 wt% GI- POSS TMF	-	307	(14)	560	12
4 wt% GI- POSS TMF	196	314	-	527	19
6 wt% GI- POSS TMF	199	312	(8)	520	13

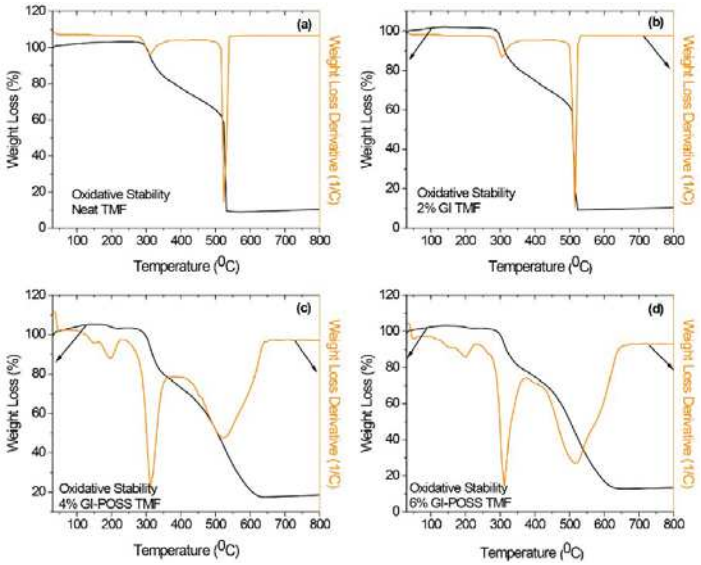

Fig. (5). Thermal oxidative stability curves for (**a**) neat TMF (**b**) 2% GI-POSS TMF (**c**) 4% GI-POSS TMF, and (**d**) 6% GI-POSS TMF. (*A higher resolution / colour version of this figure is available in the electronic copy of the article*).

Table 3. TMA data for neat and EC-POSS TMF.

Sample	CTE Before Tg (μm)	Δ (%)	Tg (°C)	CTE After Tg	Δ (%)
Neat TMF	-3.738	----	106	1684	----
2 wt% EC-POSS TMF	-5.864	-56.9	110	1274	24.3
4 wt% EC-POSS TMF	-11.72	-214	110	983.3	41.6
6 wt% EC-POSS TMF	-10.78	-188	110	863	48.7

and 48% decrease in CTE (Coefficient of Thermal Expansion) for 2 and 6 wt% EC-POSS TMF, respectively, compared to the neat TMF, with no change in T_g. As expected, the T_g values measured for neat TMF and EC-POSS infused TMF showed no significant changes. The T_g values were ~106-110°C within the range of experimental error.

(Fig. **6**) shows the reduced stress-strain curves for the neat TMF and EC-POSS TMF. The test results are summarized in Table **4**. These results clearly show that the maximum increase in strength and modulus was ~ 33 and 120%, respectively, for the 4 wt% EC-POSS TMF. The 6 wt% EC-POSS TMF showed only a 28% increase in strength and a 73% increase in modulus, as compared to the neat TMF. These results also show that the higher percentage (>6 wt %) of EC-POSS TMF resulted in a decrease in properties. This change may have been due to particle-particle interactions rather than particle-polymer interactions.

The compressive properties studied for the EC-POSS and GI-POSS systems with 2, 4, and 6 wt% infusion in TMF showed an increase in strength and modulus for the 2 and 4 wt% infusions. The highest increase in strength and modulus was exhibited by 4 wt% GI-POSS TMF. The 4 wt% EC-POSS TMF showed a simultaneous increase in strength and modulus. These results clearly show that the selection of the best system depends on the required properties. Based on this study and thermal stability study, the 4 wt% GI-POSS TMF displayed the highest strength, highest modulus, and better thermal stability among all the TMF systems. So, we selected 4 wt% GI-POSS TMF to be used for the sandwich foam core material.

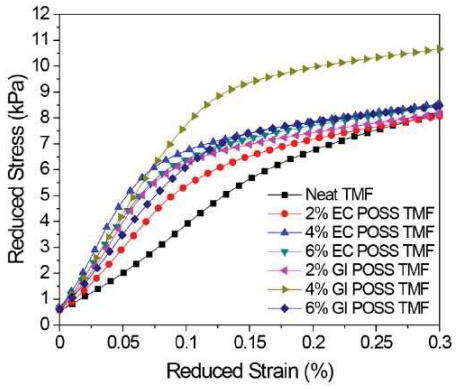

Fig. (6). Quasi-static compression curves for neat, EC-, and GI-POSS TMF. (*A higher resolution / colour version of this figure is available in the electronic copy of the article*).

Table 4. Quasi-static compression data for neat, EC-POSS, and GI-POSS TMF.

Sample	Reduced Compression Strength (kPa/kg *m^{-3})	% Increase	Reduced Compression Modulus (MPa/kg *m^{-3})	% Increase
Neat TMF	5.681	-	0.044	-
2 wt% EC- POSS TMF	6.772	19	0.071	61
4 wt% EC- POSS TMF	7.564	33	0.097	120
6 wt% EC- POSS TMF	7.252	28	0.076	73
2 wt% GI- POSS TMF	7.207	27	0.117	165
4 wt% GI- POSS TMF	9.163	61	0.130	195
6 wt% GI- POSS TMF	8.250	45	0.114	159

(Fig. **7**) depicts the TMA results for Neat 8612, and 0.5 and 1 wt% CNTs and EC-POSS/CNTs infused in 8612; the results are summarized in Table **5**. These results clearly show that 3.3, 19 and 16% decrease in CTE for 0.5 wt% EC-POSS/CNTs and 1 wt% EC-POSS/CNTs infused systems as compared to the neat 8612 system. The CTE values measured the T_g temperature increased (from 18.3 to 18.86µm) slightly for 1.0% EC-POSS infused system. The T_g values measured for these systems showed no significant changes. The T_g values were ~88-98°C within the range of experimental errors. The 1% EC-POSS/CNTs system exhibited the greatest decrease in CTE at -19%.

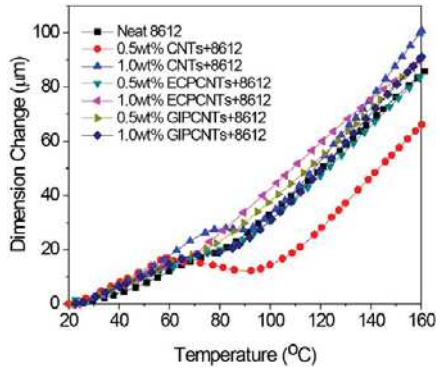

Fig. (7). TMA curves for neat, EC-, and GI-POSS nanophased Ren-Infusion 8612. (*A higher resolution / colour version of this figure is available in the electronic copy of the article*).

(Fig. **8**) shows stress-strain curves for the neat 8612, pristine CNTs, and EC-POSS/CNTs. The test results are summarized in Table **6**. For the EC-POSS CNTs, the modulus increased for all of the samples. The highest increases were observed with the 1 wt% EC-POSS CNTs system, with an increase in strength and modulus of 5 and 73%, respectively, compared to the neat sample values. The 1 wt% EC-POSS system showed a similar increase in strength compared to the 1 wt% EC-POSS/CNTs system. Small increases in the strength were exhibited except for the 0.5 wt % EC-POSS system, which shows -2% change in the strength.

(Fig. **8**) shows stress-strain curves for the neat 8612, pristine CNTs, GI-POSS/CNTs, and GI-POSS infused 8612 with the test results summarized in Table **6**. All GI-POSS CNT samples exhibited an increase in modulus. The greatest increase in modulus of ~41% was exhibited by 1.0 wt% GI-POSS/CNTs. The 1.0 wt% GI-POSS exhibited the highest increase in strength at 4%. A similar trend was observed for the EC-POSS nanophased systems. Decreases in strength were observed for the 0.5 wt% GI-POSS CNTs and GI-POSS as well as the 1 wt% GI-POSS CNTs.

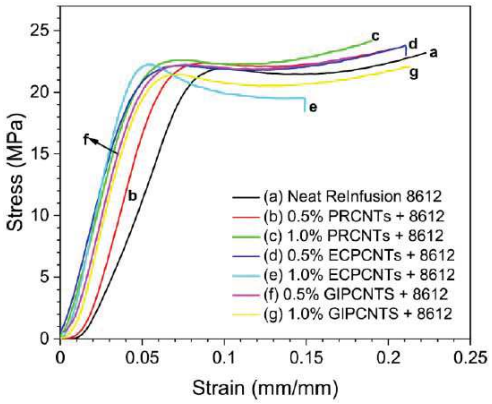

Fig. (8). Quasi-static compression curves for neat, EC-POSS, and GI-POSS carbon nanotubes. (*A higher resolution / colour version of this figure is available in the electronic copy of the article*).

3.3. Neat and Nanophased Sandwich Panels

Neat and nanophased sandwich panels were constructed after all TMF and nanophased resin system properties were evaluated. From those results discussed previously, it was determined that the 4wt% GI-POSS TMF exhibited the highest strength, highest modulus and better thermal stability and thus selected for the foam core material. For the nanophased resin, 1 wt% EC POSS CNTs exhibited the best properties to use as a face sheet of the sandwich structure. Because the sample sizes were quite large, only optical micrographs were taken for both panels. (Figs. **10** and **11**) show optical micrographs of the neat and nanophased panels before compression evaluation.

The flatwise compressive properties of the sandwich panels were determined according to the standard method ASTM C365. A total of 5 square specimens with dimensions of 25.4 mm (1 in) x 25.4 mm (1 in) were cut from the sandwich panels. The specimens were tested using an MTS machine with a total capacity of ± 220 kips and monotonically loaded in compression up to failure. The typical stress-

Table 5. TMA data for neat, EC-POSS, and GI-POSS nanophased RenInfusion 8612.

Sample	CTE (µm)	Δ (%)	$(T_g)^{\circ}C$
Neat ReInfusion 8612	18.3	----	95
0.5 wt% CNT+8612	26.1	+43	95
1.0 wt% CNT+8612	25.56	+39	92
0.5 wt% EC-POSS/CNT+8612	17.7	-3.3	90
1.0 wt% EC-POSS/CNT+8612	14.9	-19	97
0.5 wt% GI-POSS/CNT+8612	18.35	+0.2	82
1.0 wt% GI-POSS/CNT+8612	15.8	-14	96

Table 6. Quasi-static compression data for neat, EC-POSS, and GI-POSS RenInfusion 8612.

Sample	Max Compression Strength (MPa)	% Increase	Compression Modulus (MPa)	% Increase
Neat RenInfusion 8612	21.92±0.16	-	354±97	-
0.5 wt% PRCNTs	22.37±0.08	2	446±15	26
1.0 wt% PRCNTs	22.59±0.12	3	463±32	31
0.5 wt% EC-POSS/CNTs	22.10±0.05	1	532±26	50
1.0 wt% EC-POSS/CNTs	22.99±0.01	5	613±2	73
0.5 wt% GI-POSS CNTs	21.2±0.03	-3	364±44	3
1.0 wt% GI-POSS CNTs	21.3±0.05	-3	500±25	41

strain relationship of the tested compression sandwich specimens is shown in Fig. (**9**) and the data are summarized in Table **7**. Test results showed that the compressive modulus for the neat sandwich panel was 15.96 MPa while the nanophased sandwich panel had a compressive modulus of 17.35 MPa. The compressive strengths of the neat and nanophased sandwich panels were 0.503 and 0.486 MPa, respectively. The nanophased panel exhibited a slight decrease of 3% in the strength compared to the neat.

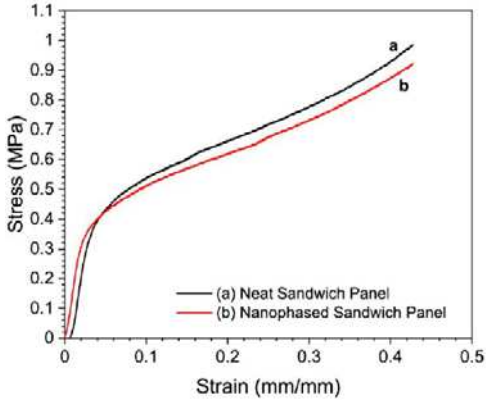

Fig. (9). Average stress/strain curves for sandwich panels. (*A higher resolution / colour version of this figure is available in the electronic copy of the article*).

Table 7. Compressive properties for sandwich panels.

Structure	Compressive Strength (MPa)	Compressive Modulus (MPa)
Neat Sandwich Panel	0.503 ±0.023	15.961 ±0.006
Nanophased Sandwich Panel	0.486 ±0.002	17.345 ±0.005

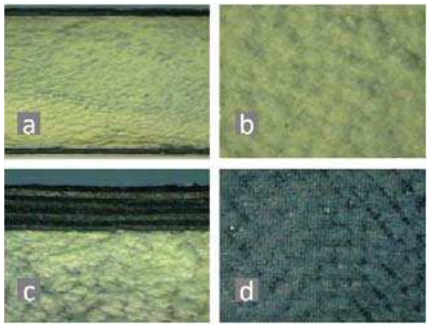

Fig. (10). Neat sandwich panel before quasi-static compression evaluation: (**a**) overall view; (**b**) side view; (**c**) middle foam core; (**d**) top face sheet view. (*A higher resolution / colour version of this figure is available in the electronic copy of the article*).

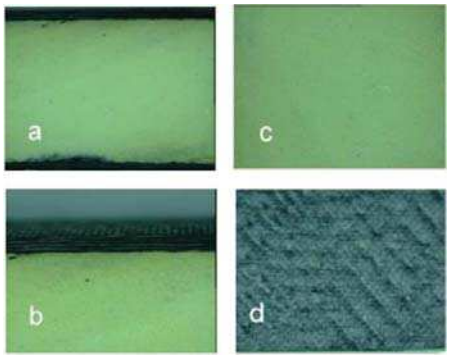

Fig. (11). Nanophased sandwich panel before quasi-static compression evaluation: (**a**) overall view; (**b**) side view; (**c**) middle foam core; (**d**) top face sheet view. (*A higher resolution / colour version of this figure is available in the electronic copy of the article*).

Following the compression tests, the failure modes in the samples were revealed using a low power optical microscope. From the micrographs presented in Figs. (**12a**, **12b**, and **12c**), it was apparent that several modes of failure were observed in neat sandwich structures. The initial failure took the form of a buckling failure in the uppermost skin of the sandwich structure. A similar mode of failure was observed, resulting from shear cracking through the depth of the core material. If the core is very brittle, initial failure is likely to take the form of shear cracking through the thickness of the foam.

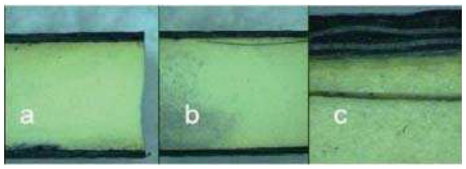

Fig. (12). Neat sandwich panel after quasi-static compression evaluation: (**a**) overall view; (**b**) side 2 view with crack; (**c**) higher magnification of crack. (*A higher resolution / colour version of this figure is available in the electronic copy of the article*).

In the case of the nanophased sandwich panel (Fig. **13**), only buckling in the foam core was observed. No cracks were seen. This was an indication that the nanofillers could have contributed to crack resistance in the materials.

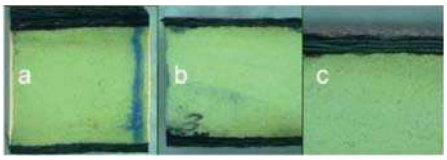

Fig. (13). Nanophased sandwich panel after quasi-static compression evaluation: (**a**) overall view; (**b**) side 2 view; (**c**) higher magnification. (*A higher resolution / colour version of this figure is available in the electronic copy of the article*).

CONCLUSION

A novel sonochemical method was adapted to incorporate CNTs and POSS nanoparticles into a sandwich composite structure. Thermal analysis showed an increase in thermal stability for the POSS infused TMFs. TMA analyses revealed no significant change in the glass transition temperature, however, decreases in the CTE before and after the glass transition temperature was observed. Increases in the compressive strength and modulus were observed for nanophased TMFs compared to the as-prepared TMF. Overall improvements in thermal and mechanical properties were observed for 4 wt% GI-POSS TMF. Quasi-static compression results indicated significant increases (73%) in compressive modulus, and an increase (5%) in compressive strength for the 1 wt% EC-POSS/CNTs resin system. The nanophased sandwich structure constructed from the 1 wt% EC-POSS/CNTs resin system as a face sheet and the 4 wt% GI-POSS TMF as a core material displayed an increase (9%) in modulus over the neat sandwich structure. Cracking and buckling were observed in the neat sandwich composite. The nanophased sandwich panel exhibited only buckling in the foam core. Finally, the excellent mechanical and thermal properties of the nanophased sandwich panels as compared to neat sandwich panel suggested that nanophase panels could serve as excellent candidates for applications in boats, ships, high-performance aerospace vehicles, and rail cars structures.

ETHICS APPROVAL AND CONSENT TO PARTICIPATE

Not applicable.

HUMAN AND ANIMAL RIGHTS

No Animals/Humans were used for studies that are base of this research.

CONSENT FOR PUBLICATION

Not applicable.

AVAILABILITY OF DATA AND MATERIALS

The authors confirm that the data supporting the research findings of this study are available within the article and will be provided upon request

FUNDING

The authors would like to acknowledge the financial support of the National Science Foundation NSF-CREST#1137681, NSF-RISE #1459007 grants. We also acknowledge the support from Alabama EPSCoR, and Alabama Commission on Higher Education for financial support and Expancel Inc. for providing polymeric samples.

CONFLICT OF INTEREST

The authors confirm that this article content has no conflict of interest.

ACKNOWLEDGEMENTS

The authors would like to thank the NSF-IGERT, NSF-PREM, Alabama EPSCoR, and Alabama Commission on Higher Education for financial support and Expancel Inc. for providing polymeric samples. .

REFERENCES

[1] Mallick PK. Fiber-reinforced composites. (2nd ed.), New York, NY: Marcel Dekker Inc. 1993.
[2] Agarwal BD, Broutman LJ. Analysis and performance of fiber composites. (2nd ed.), Hoboken, NJ: Wiley 1990.
[3] Ashland D, Pradeep P. The Science and Engineering of Materials. (5th ed.), Thompson Canada 2006.
[4] AMD. Olsson KA. Sandwch structures for naval ships: design and experienceMechanics of Sandwich Structures. ASME 2000; 62: pp. 1-9.
[5] Osei-Antwi M, De Castro J, Vassilopoulos AP, Keller T. Shear mechanical characterization of balsa wood as core material of composite sandwich panels. Constr Build Mater 2013; 41: 231-8. http://dx.doi.org/10.1016/j.conbuildmat.2012.11.009

[6] Hassanin AH, Hamouda T, Candan Z, Kilic A, Akbulut T. Developing high-performance hybrid green composites. Compos, Part B Eng 2016; 92: 384-94. http://dx.doi.org/10.1016/j.compositesb.2016.02.051

[7] Hamouda T, Hassanin AH, Saba N, *et al.* Evaluation of mechanical and physical properties of hybrid composites from food packaging and textiles wastes. J Polym Environ 2019; 27: 489-97. http://dx.doi.org/10.1007/s10924-019-01369-3

[8] Hosur MV, Mohammed AA, Zainuddin S, Jeelani S. Processing of nanoclay filled sandwich composites and their response to low–velocity impact loading. Comp Struct 2008; 82: 101-16. http://dx.doi.org/10.1016/j.compstruct.2006.12.009

[9] Kabir ME, Saha MC, Jeelani S. Effect of ultrasound sonication in carbon nanofibers/polyurethane foam composite. Mater Sci Eng A 2007; 459: 111-6. http://dx.doi.org/10.1016/j.msea.2007.01.031

[10] Zainuddin S, Mahfuz H, Jeelani S. Enhancing fatigue performance of sandwich composites with nanophased core. J Nanomater 2010; ••• http://dx.doi.org/10.1155/2010/712731

[11] Mahfuz H, Uddin MF, Rangari VK, Saha MC, Zainuddin S, Jeelani S. High strain rate response of sandwich composites with nanophased cores. Appl Compos Mater 2005; 12: 193-211. http://dx.doi.org/10.1007/s10443-005-1123-5

[12] Mahfuz H, Islam M, Rangari V, Saha M, Jeelani S. Response of sandwich composites with nanophased cores under flexural loading. Compos Part B 2005; 35: 543-50. http://dx.doi.org/10.1016/j.compositesb.2003.11.004

[13] Hamouda T, Hassanin AH, Kilic A, Candan Z, Bodur MS. Hybrid composites from coir fibers reinforced with woven glass fabrics: physical and mechanical evaluation. Polym Compos 2017; 38(10): 2212-20. http://dx.doi.org/10.1002/pc.23799

[14] Mahfuz H, Rangari V, Islam M, Jeelani S. Fabrication, synthesis and mechanical characterization of nanoparticles infused polyurethane foams. Compos Part A 2004; 35: 453-60. http://dx.doi.org/10.1016/j.compositesa.2003.10.009

[15] Shifa M, Tariq F, Baloch R. Effect of Carbon Nanotubes on mechanical properties of honeycomb sandwich panels. Nucleus 2017; 54(1): 1-6.

[16] Rangari V, Hassan T, Zhou Y, Mahfuz H, Jeelani S, Prorok B. Cloisite clay-infused phenolic foam nanocomposites. J Appl Polym Sci 2007; 103: 308-14. http://dx.doi.org/10.1002/app.25287

[17] Rangari V, Jeelani MI, Zhou Y, Jeelani S. Fabrication and characterization of MWCNT/thermoplastic microsphere nanocomposite foams. Int J Nanosci 2008; 7: 161-9. http://dx.doi.org/10.1142/S0219581X08005237

[18] Uddin MN, Gandy HT, Rahman MM, Asmatulu R. Adhesiveless honeycomb sandwich structures of prepreg carbon fiber composites for primary structural applications. Advanced Composites and Hybrid Materials 2019; 2(2): 339-50. http://dx.doi.org/10.1007/s42114-019-00096-6

[19] Di Sciuva M, Sorrenti M. Bending, free vibration and buckling of functionally graded carbon nanotube-reinforced sandwich plates, using the extended Refined Zigzag Theory. Compos Struct 2019; 227 http://dx.doi.org/10.1016/j.compstruct.2019.111324

[20] Pielichowski K. Adv Polym Sci 2006; 201: 225-96. http://dx.doi.org/10.1007/12_077

[21] Harris PJF. Carbon nanotubes and related structures: new materials for the twenty –first century. Cambridge, UK: Cambridge University Press 1999. http://dx.doi.org/10.1017/CBO9780511605819

[22] Armstrong W, Sapkota B, Mishra S. Silver decorated carbon nanospheres as effective visible light photocatalyst. MRS Online Proceedings Library Archive 2013; p. 1509.

[23] Joshi M, Butola BS. Polymeric nanocomposites: polyhedral oligomeric silsesquioxanes (POSS) as hybrid nanofiller. J Macromol Sci: Part C 2004; 44: 389-410. http://dx.doi.org/10.1081/MC-200033687

[24] Jung Y, Sahoo NG, Cho JW. Polymeric nanocomposites of polyurethane block copolymers and functionalized multi-walled carbon nanotubes as crosslinkers. Macromol Rapid Commun 2006; 27: 126-31. http://dx.doi.org/10.1002/marc.200500658

[25] Dohi H, Kikuchi S, Kuwahara S, Sugai T, Shinohara H. Synthesis and spectroscopic characterization of single-wall carbon nanotubes wrapped by glycoconjugate polymer with bioactive sugars. Chem Phys Lett 2006; 428: 98-101. http://dx.doi.org/10.1016/j.cplett.2006.06.053

[26] Baskaran D, Mays JW, Bratcher MS. Noncovalent and nonspecific molecular interactions of polymers with multiwalled carbon nanotubes. Chem Mater 2005; 17: 3389-97. http://dx.doi.org/10.1021/cm047866e

[27] Konyushenko EN, Stejskal J, Trchova M, *et al.* Multi-wall carbon nanotubes coated with polyaniline. Polymer (Guildf) 2006; 47: 5715-23. http://dx.doi.org/10.1016/j.polymer.2006.05.059

[28] Rivin D, Suzin Y. Calorimetric investigation of the interaction of carbon nanotubes with polystyrene. J Polym Sci: Part B 2006; 44: 1821-34. http://dx.doi.org/10.1002/polb.20831

[29] Zhang R, Wang X. One step synthesis of multiwalled carbon nanotube/gold nanocomposites for enhancing electrochemical response. Chem Mater 2007; 19: 976-8. http://dx.doi.org/10.1021/cm062791v

[30] Bittencourt C, Felten A, Ghijsen J, *et al.* Decorating carbon nanotubes with nickel nanoparticles. Chem Phys Lett 2007; 436: 368-72. http://dx.doi.org/10.1016/j.cplett.2007.01.065

[31] Kong H, Li W, Gao C, *et al.* Poly(N-isopropylacrylamide)-coated carbon nanotubes: temperature sensitive molecular nanohybrids in water. Macromolecules 2004; 37: 6683-6. http://dx.doi.org/10.1021/ma048682o

[32] Franchini E, Galy J, Gerard JF, Tabuani D, Medici A. Influence of POSS structure on the fire retardant properties of epoxy hybrid networks. Polym Degrad Stabil 2009; 4: 1728-36. http://dx.doi.org/10.1016/j.polymdegradstab.2009.06.025

[33] Du W, Shan J, Wu Y, Xu R, Yu D. Preparation and characterization of polybenzoxazine/trisilanol polyhedral oligomeric silsesquioxanes composites. Mater Des 2010; 31: 1720-5. http://dx.doi.org/10.1016/j.matdes.2009.01.050

[34] Ni C, Ni G, Zhang S, Liu X, Chen M, Liu L. The preparation of inorganic/organic hybrid nanomaterials containing silsesquioxane and its reinforcement for an epoxy resin network. Colloid Polym Sci 2010; 288: 469-77. http://dx.doi.org/10.1007/s00396-009-2160-7

[35] Zhang Z, Gu A, Liang G, Ren P, Xie J, Wang X. Thermo-oxygen mechanisms of POSS/epoxy nanocomposites. Polym Degrad Stabil 2009; 92: 1986-93. http://dx.doi.org/10.1016/j.polymdegradstab.2007.08.004

[36] Qiu Z, Pan H. Preparation, crystallization and hydrolytic degradation of biodegradable poly(L-lactide)/polyhedral oligomeric silsesquioxanes nanocomposites. Compos Sci Technol 2010; 70: 1089-94. http://dx.doi.org/10.1016/j.compscitech.2009.11.001

[37] Su CH, Chiu YP, Teng CC, Chiang CL. Preparation, characterization and thermal properties of organic–inorganic composites involving epoxy and polyhedral oligomeric silsesquioxane (POSS) J Polym Res 2010; 17: 673-81. http://dx.doi.org/10.1007/s10965-009-9355-y

[38] ASTM Standard E831. Standard Test Method for Linear Thermal Expansion of Solid Materials by Thermomechanical Analysis ASTM International 2003; 17: 673-81. http://dx.doi.org/10.1007/s10965-009-9355-y

[39] ASTM Standard C365. Standard Test Method for Flatwise Compressive Properties of Sandwich Cores ASTM International 2003. http://dx.doi.org/10.1007/s10965-009-9355-y

[40] Mao Q, Yang L, Geng X, Chen L, Zhao H, *et al.* Interface Strain Induced Hydrophobic Facet Suppression in Cellulose Nanocomposite Embedded with Highly Oxidized Monolayer Graphene Oxide. Adv Mater Interfaces 2017; 4(23) http://dx.doi.org/10.1002/admi.201700995

[41] Bhoyate S, Kahol PK, Mishra SR, Perez F, Gupta RK. Polystyrene activated linear tube carbon nanofiber for durable and high-

-performance supercapacitors. Surf Coat Tech 2018; 345: 113-22. http://dx.doi.org/10.1016/j.surfcoat.2018.04.026